

Supporting Information

Backbone distortions in lactam-bridged helical peptides

Ali Moazzam,^{‡+a} Vesna Stanojlovic,^{‡a} Arthur Hinterholzer,^a Christoph Holzner,^a Cornelia Roschger,^b Andreas Zierer,^b Markus Wiederstein,^a Mario Schubert^{*a} and Chiara Cabrele^{*a}

^a Department of Biosciences, Paris Lodron University of Salzburg, 5020 Salzburg, Austria.

^b Department for Cardiac-, Vascular- and Thoracic Surgery, Johannes Kepler University Linz and Kepler University Hospital GmbH, 4020 Linz, Austria.

[‡] The authors contributed equally to this work.

⁺ Current address: School of Chemistry, College of Science, University of Tehran, P.O. Box 14155-6619, Tehran

* Corresponding author: Email: chiara.cabrele@plus.ac.at. Co-corresponding author: Email: mario.schubert@plus.ac.at.

Materials

Chemical reagents and solvents for the peptide syntheses were of peptide-synthesis grade; solvents for HPLC and spectroscopy were of HPLC or spectroscopy grade. Fmoc-protected amino acids, Rink-amide MBHA resin (100-200 mesh, loading 0.57 mmol/g), N,N-diisopropylethylamine (DIPEA), piperidine, N,N-dimethylformamide (DMF), N-methyl-2-pyrrolidone (NMP), dichloromethane (DCM), diethylether and trifluoroacetic acid (TFA) were purchased from Iris Biotech (Germany). Thioanisole (TIA), acetic anhydride, PhSiH₃, Pd(PPh₃)₄, acetonitrile, α -cyano-4-hydroxycinnamic acid, triisopropylsilane (TIS) and 1,2-ethanedithiol (EDT) were purchased from Sigma Aldrich (Germany). 2-(1H-benzotriazole-1-yl)-1,1,3,3-tetramethyluronium hexafluorophosphate (HBTU) and N-hydroxybenzotriazole (HOBT) were purchased from Biosolve (The Netherlands). D₂O was from Armar GmbH (Germany). 3-(4,5-Dimethylthiazol-2-yl)-2,5-diphenyltetrazolium bromide (MTT), fetal bovine serum, penicillin–streptomycin and L-glutamine were purchased from Sigma-Aldrich (Austria). Dulbecco's modified Eagle's medium (DMEM)–high glucose and Roswell Park Memorial Institute (RPMI) 1640 medium were purchased from Szabo-Scandic (Austria). Dimethyl sulfoxide (DMSO) was from VWR (Austria). The primary human lung fibroblasts were a gift from Prof. Dr. Jutta Horejs-Höck, University of Salzburg (Austria). The cell line MCF-7 was a gift from Prof. Dr. Barbara Krammer, University of Salzburg (Austria). The cell lines HT1975, A427 and SKLU-1 were a gift from Prof. Dr. Emilio Casanova, Medical University of Vienna (Austria). The cell lines A549 (ATCC: CLL-185), H460 (ATCC: HTB-177), H520 (ATCC: HTB-182) and HCC827 (ATCC: CRL-2868) were purchased from ATCC.

Methods

Solid-phase peptide synthesis was carried out on an automatic peptide synthesizer (Syro I, Biotage). The analytical HPLC equipment was from Thermo Fisher Scientific (Ultimate 3000). The analytical column was from Thermo Fisher Scientific (Synchronis C₁₈, 4.6x250 mm). The gradient used for analytical HPLC was the following: 3% B for 8 min, up to 60% B over 35 min (A = H₂O with 0.06% TFA; B = CH₃CN with 0.05% TFA). MALDI-TOF mass spectra were recorded on an Autoflex mass spectrometer from Bruker Daltonics using α -cyano-4-hydroxycinnamic acid as matrix. The CD measurements were recorded on a Chirascan Plus CD spectrometer from Applied Photophysics. UV measurements were carried out on a Varian Cary UV-visible spectrophotometer. For the determination of the cell viability with the MTT assay, a GloMax® Multimode Microplate Reader was used.

Cell-viability assay

The primary human lung fibroblast and the MCF-7 cell line were cultured in DMEM–high glucose supplemented with 10% fetal bovine serum, 1% penicillin–streptomycin and 1% L-glutamine. All other cell lines were maintained in RPMI 1640 medium supplemented with 10% fetal bovine serum, 1% penicillin–streptomycin and 1% L-glutamine. Cells were grown in a humidified atmosphere at 37 °C in 5% CO₂. For all experiments, 70–80% confluent cells were used. Cells (10000 cells/well) in complete growth medium were seeded into 96-well culture plates. The day after, the medium was changed to a serum free medium with peptides at a concentration of 100 µM. After an additional incubation period of 24 h, the cell viability was determined by adding 10 µl MTT solution (5 mg/ml in PBS) to the treated and untreated control cells for 2 h at 37 °C in the dark. Then, the medium was aspirated, the cells were lysed with 100 µl DMSO and the absorbance of the resulting product formazan in viable cells was measured at 550 nm. Three independent experiments (with each sample in triplicate) were performed and cell viability was normalized to the untreated control.

Figures

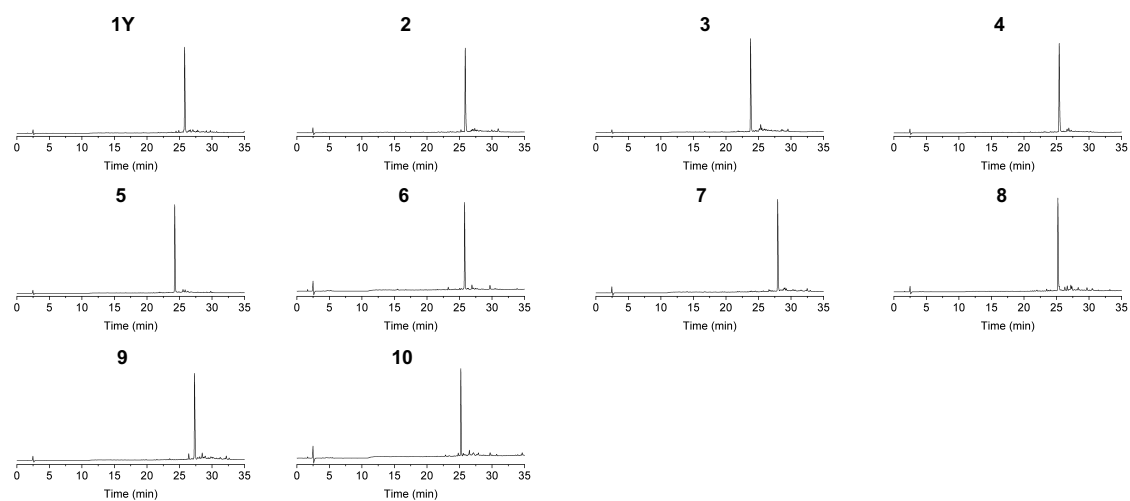


Figure S1. Analytical HPLC of the synthetic lactam-bridged peptides used in this work (see Table S1 for t_R values and gradient).

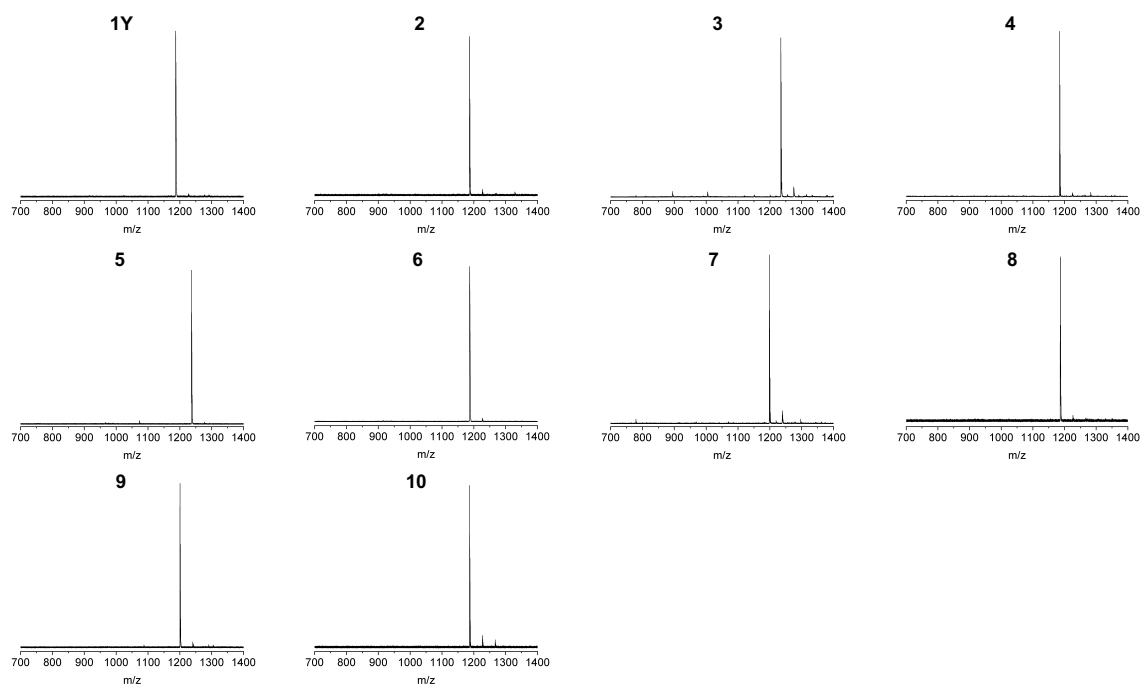


Figure S2. MALDI-TOF-MS of the synthetic lactam-bridged peptides used in this work (see Table S1 for M_{found}).

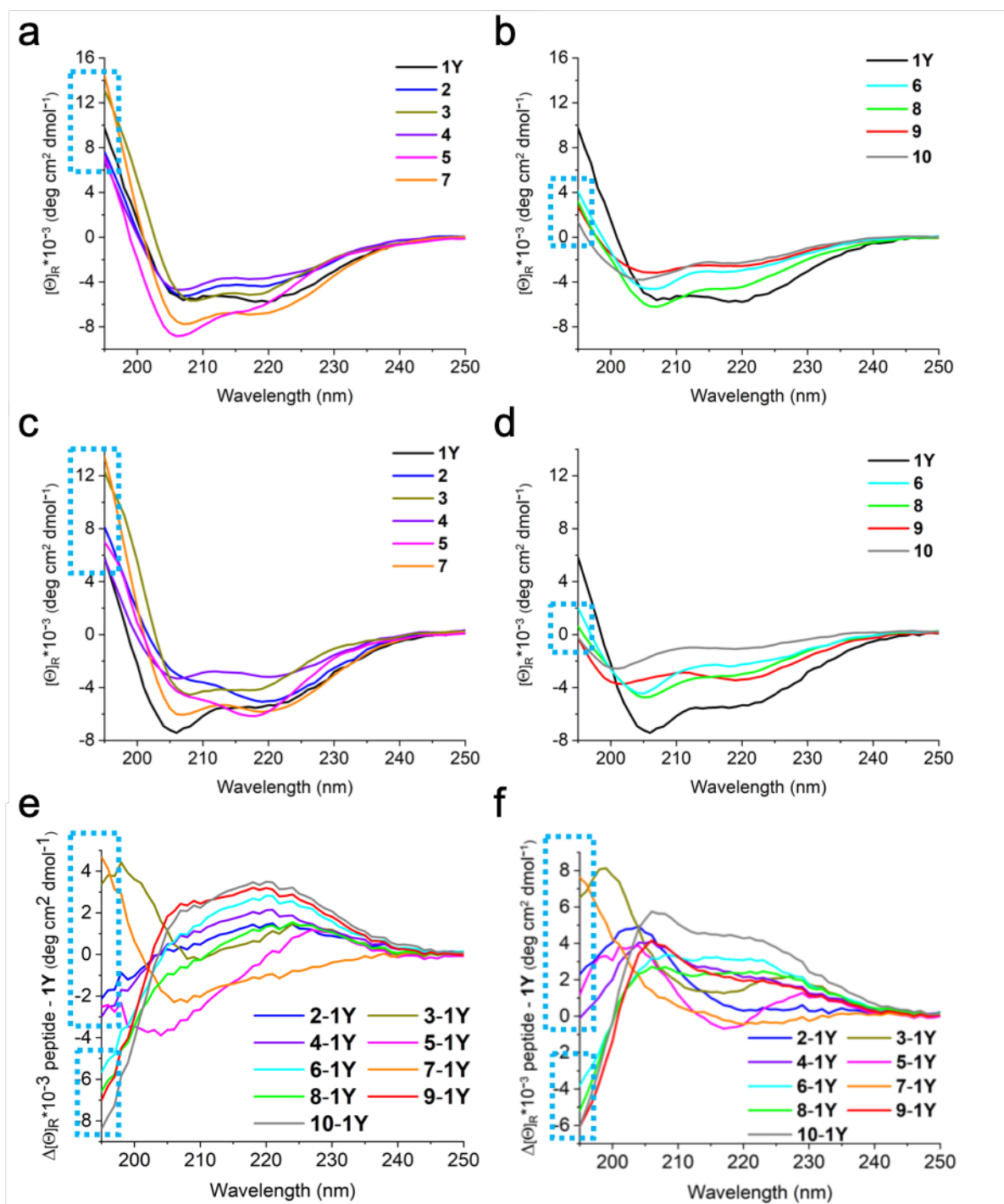


Figure S3. CD spectra of the lactam-bridged peptides in (a, b) phosphate buffer (50 mM, pH 7.3) and (c, d) water (pH range 3-4). The dashed boxes show the maximal CD contribution below 200 nm, which is higher than 6000 deg cm² dmol⁻¹ for **1Y**, **2-5**, **7** (a, c), and smaller than 4000 deg cm² dmol⁻¹ for **6**, **8-10** (b, d). Difference spectra (peptide – **1Y**) in (e) phosphate buffer and (f) water.

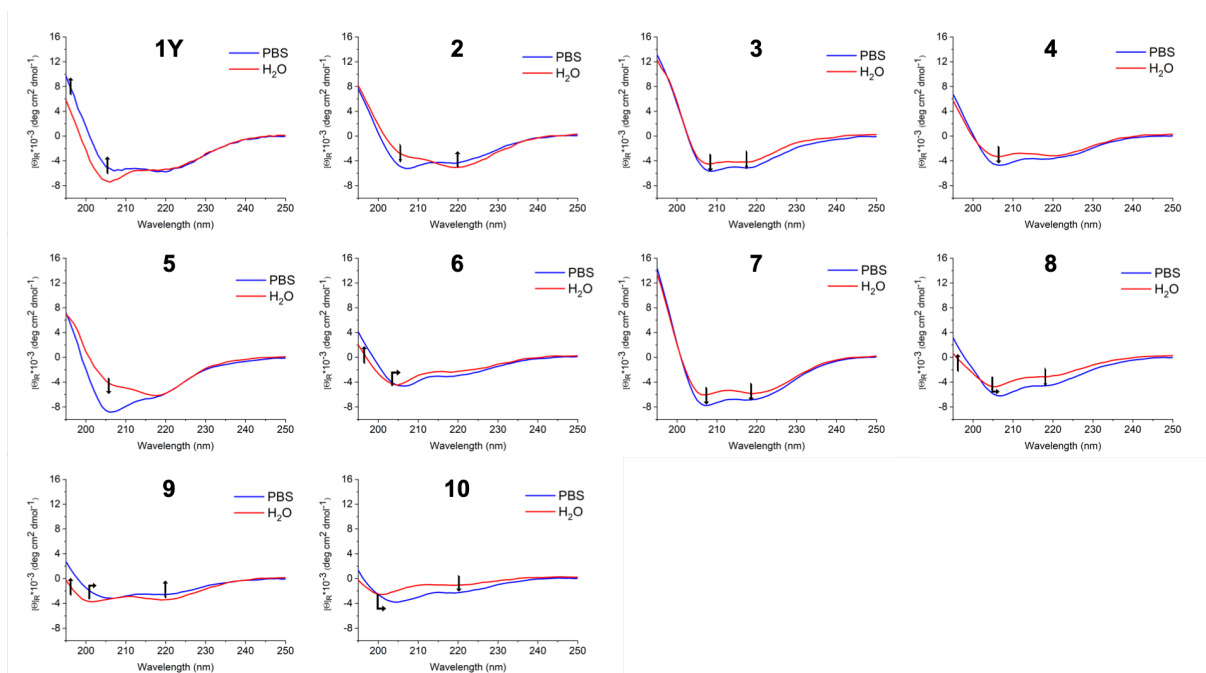


Figure S4. Comparison of the CD spectra of the lactam-bridged peptides in phosphate buffer (50 mM, pH 7.3) and water (pH range 3-4).

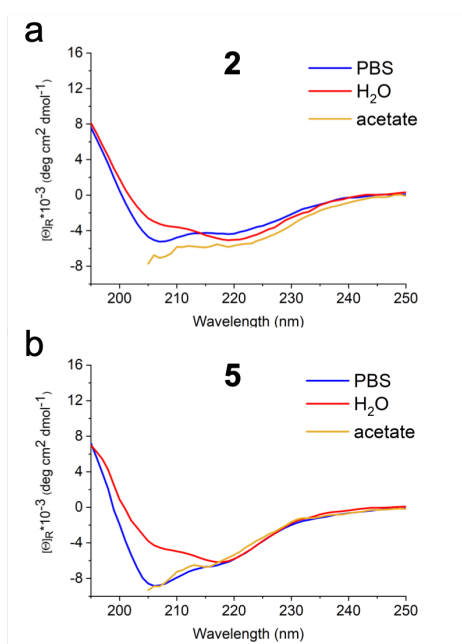


Figure S5. Comparison of the CD spectra of the lactam-bridged peptides **2** and **5** in phosphate buffer (50 mM, pH 7.3), acetate buffer (10 mM, pH 4.5) and water (pH range 3-4).

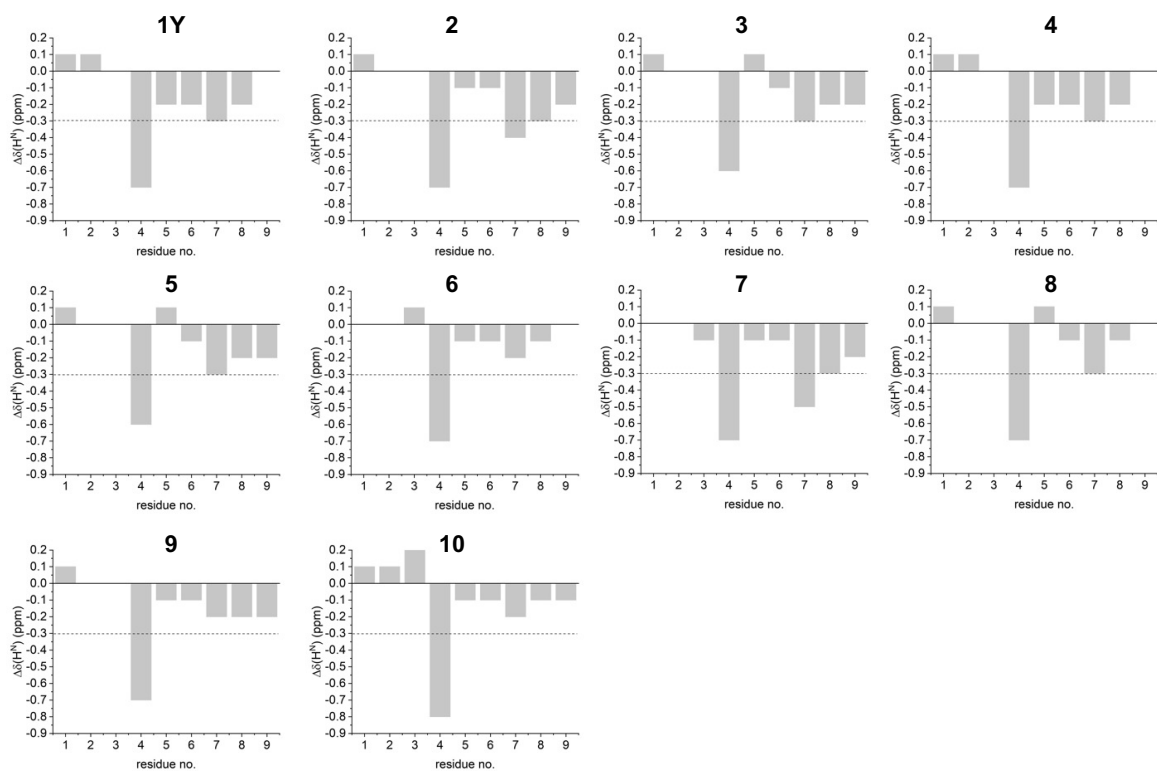


Figure S6. Chemical shifts differences (ppm) between the measured and random coil $^1\text{H}^{\text{N}}$ for each residue of the peptides in water (pH range 3-4).

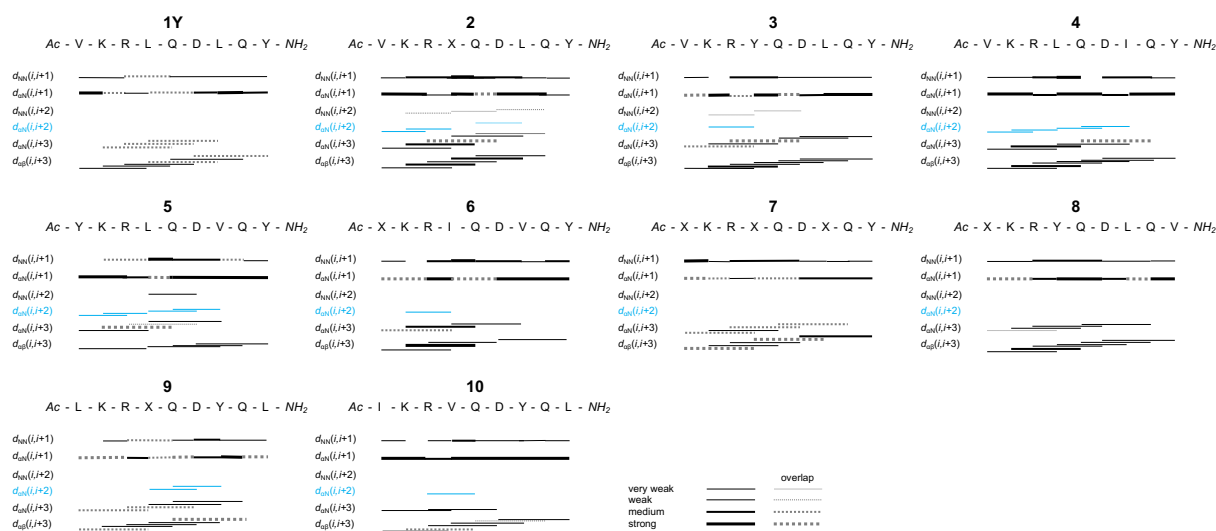


Figure S7. NOE pattern of the lactam-bridged peptides in water (pH range 3-4).

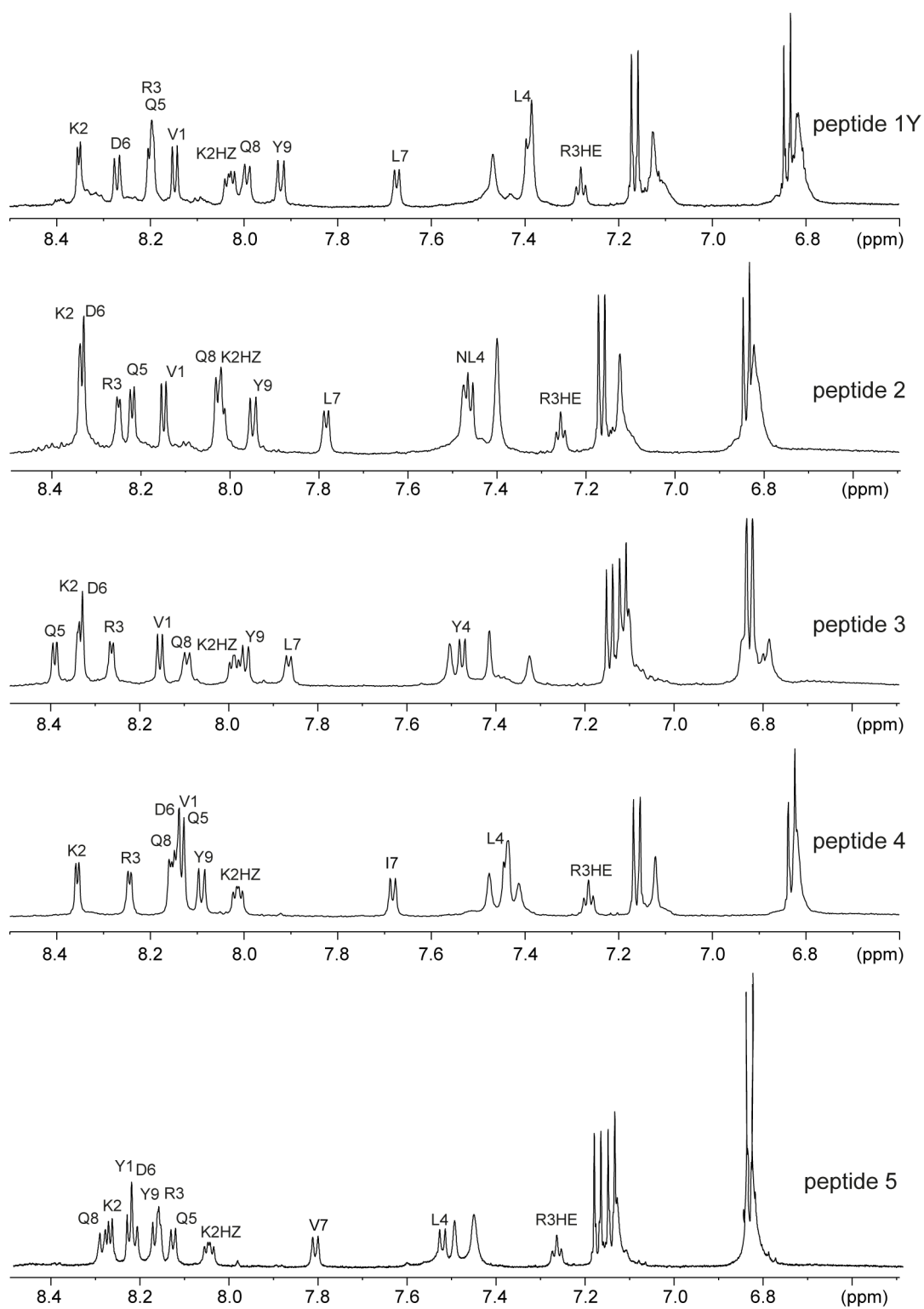


Figure S8. 1D-NMR spectra of the lactam-bridged peptides in water (pH range 3-4).

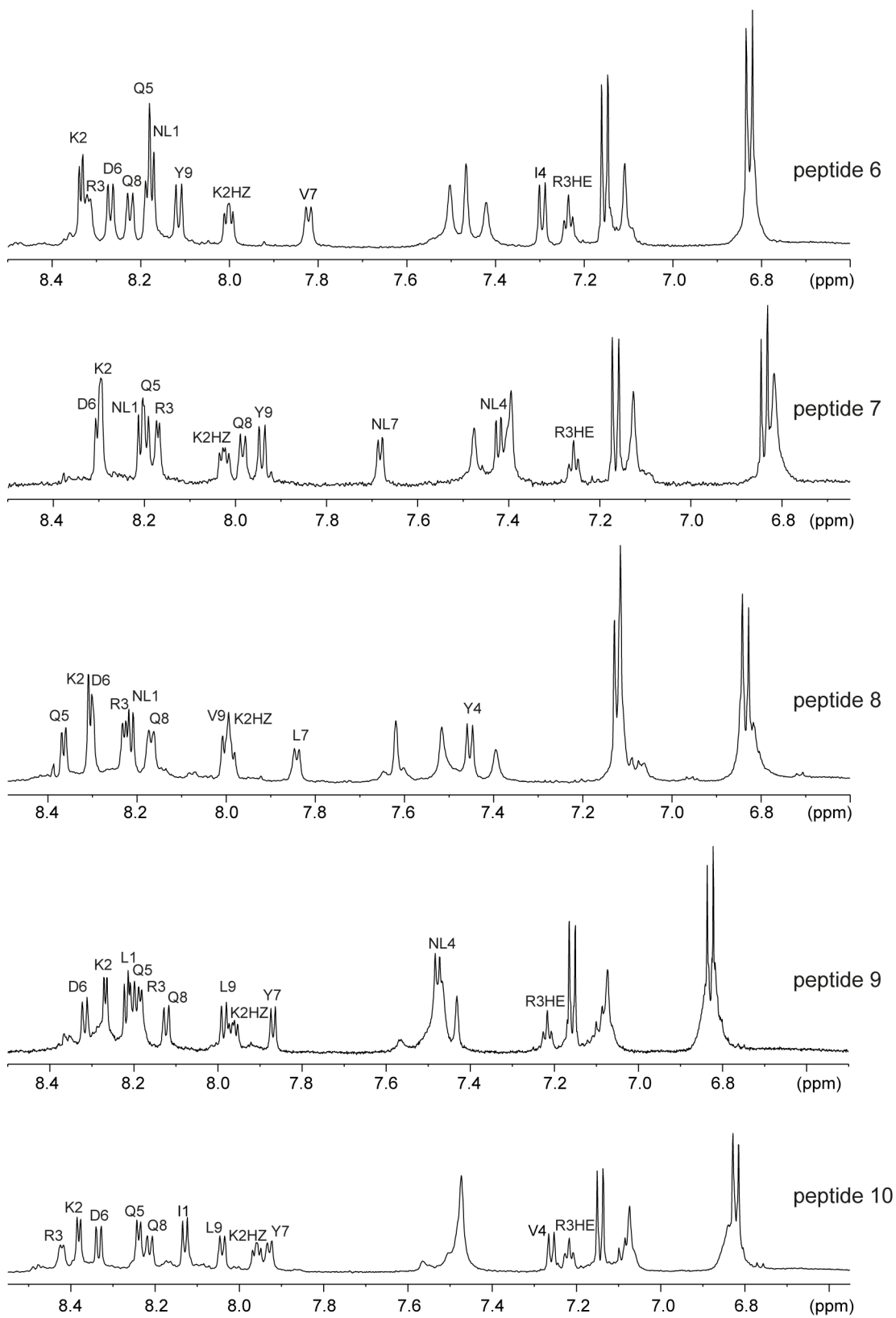


Figure S8. continued.

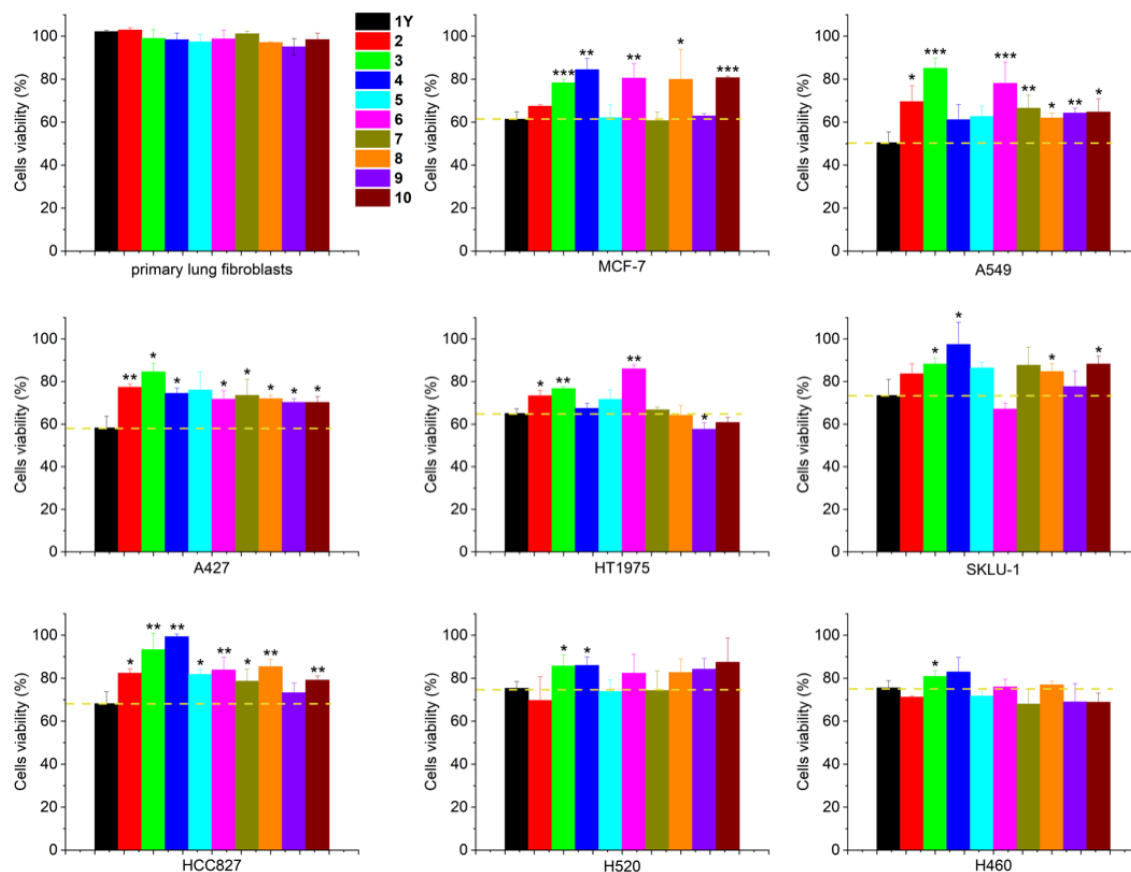


Figure S9. Effect of the lactam-bridged peptides **1Y** and **2-10** (100 μ M) on cancer-cell viability. MCF-7: human breast adenocarcinoma; A549, SKLU-1, H1975 und A427: human lung non-small cell adenocarcinoma; HCC827: human lung non-small cell adenocarcinoma with an EGFR mutation; H520: human lung squamous cell carcinoma; H460: human lung large cell adenocarcinoma. Human primary lung fibroblasts were used as control. p-Values (referred to **1Y**): ***: <0.001; **: <0.01; *: <0.05. In previous reports we showed that **1Y** reduces cancer-cell viability in the low micromolar concentration range²⁻⁴. Here, we show that none of the new analogs was more effective than **1Y**, displaying similar or reduced efficiency depending on the cell line. About the three analogs with the highest sequence similarity (**2-4**), the Tyr-4-containing analog **3** was less effective than **1Y** in all tested cell lines, whereas the Nle-4-containing analog **2** and the Ile-7-containing analog **3** were comparable to **1Y** only in four and three cell lines, respectively.

Tables

Table S1. Analytical characterization of the synthetic lactam-bridged peptides used in this work (X = Nle).

Number	Peptide sequence	M _{theor.} ^a (Da)	M _{found} ^b (Da)	t _R ^e (min)	μH ^f
1Y	cyclo-(2,6)-(Ac-VKRLQDLQY-NH ₂)	1185.40	1186.936 ^c	25.7	0.466
2	cyclo-(2,6)-(Ac-VKRXQDLQY-NH ₂)	1185.40	1186.612 ^c	25.8	0.466
3	cyclo-(2,6)-(Ac-VKRYQDLQY-NH ₂)	1235.41	1234.537 ^d	23.7	0.385
4	cyclo-(2,6)-(Ac-VKRLQDIQY-NH ₂)	1185.40	1184.557 ^d	25.4	0.470
5	cyclo-(2,6)-(Ac-YKRLQDVQY-NH ₂)	1235.41	1236.679 ^c	24.3	0.430
6	cyclo-(2,6)-(Ac-XKRIQDVQY-NH ₂)	1185.40	1186.888 ^c	25.8	0.502
7	cyclo-(2,6)-(Ac-XKRXQDXQY-NH ₂)	1199.42	1198.571 ^d	27.9	0.502
8	cyclo-(2,6)-(Ac-XKRYQDLQV-NH ₂)	1185.40	1186.756 ^c	25.2	0.409
9	cyclo-(2,6)-(Ac-LKRXQDYQL-NH ₂)	1199.42	1200.490 ^c	27.3	0.458
10	cyclo-(2,6)-(Ac-IKRVQDYQL-NH ₂)	1185.40	1186.852 ^c	25.2	0.425

a. Averaged mass

b. Measured by MALDI-TOF-MS

c. Positive mode (M+H)⁺

d. Negative mode (M-H)⁻

e. HPLC gradient: 3% B for 8 min, 3-60% in 35 min, with A = 0.06% TFA in water and B = 0.05% TFA in acetonitrile

f. The hydrophobic moment μH was calculated for the linear sequence (Leu was used for Nle) by using the web server HeliQuest (<https://heliquest.ipmc.cnrs.fr/>)⁵

Table S2. Statistics of the NMR-derived structures of the lactam-bridged peptides.

Peptide no.	1Y	2	3	4	5	6	7	8	9	10
NMR distance and dihedral restraints										
NOE distance restraints										
Total	119	168	176	163	166	161	113	186	141	147
Intraresidue	61	82	97	87	93	99	65	101	74	85
Interresidue										
Sequential ($ i-j = 1$)	36	46	55	44	49	46	32	60	40	39
Medium-range ($ i-j \leq 5$)	22	40	24	32	24	16	16	25	27	23
Long-range ($ i-j \geq 5$)	—	—	—	—	—	—	—	—	—	—
Dihedral restraints										
ϕ	5	5	4	7	7	3	7	3 ^a	7	3 ^a
ψ	5	5	4	7	7	3	7	3 ^a	7	3 ^a
Structural statistics										
Violations (mean and SD)										
No. of violated distance constraints > 0.2 Å	0.0 ± 0.0	0.0 ± 0.0	0.0 ± 0.0	0.0 ± 0.0	0.3 ± 0.4	0.0 ± 0.0	0.0 ± 0.0	0.0 ± 0.0	0.0 ± 0.0	0.6 ± 0.5
No. of violated dihedral angle constraints > 5°	1.1 ± 0.2	1.0 ± 0.0	1.0 ± 0.0	1.0 ± 0.0	0.9 ± 0.3	0.0 ± 0.0	1.0 ± 0.0	1.0 ± 0.0	1.0 ± 0.0	0.0 ± 0.0
Max. distance constraint violation (Å)	0.02 ± 0.02	0.16 ± 0.00	0.06 ± 0.01	0.08 ± 0.02	0.19 ± 0.05	0.15 ± 0.05	0.06 ± 0.00	0.12 ± 0.02	0.04 ± 0.01	0.20 ± 0.02
Max. dihedral angle violation (°)	12.9 ± 0.1	6.71 ± 0.40	9.48 ± 0.17	5.87 ± 0.45	7.99 ± 1.58	0.05 ± 0.08	5.48 ± 0.47	6.95 ± 0.56	7.37 ± 0.70	1.35 ± 0.16
Average pairwise rms deviation (Å)^b										
backbone	0.50 ± 0.23	0.29 ± 0.22	0.74 ± 0.34	0.26 ± 0.10	0.65 ± 0.24	0.77 ± 0.30	0.29 ± 0.13	0.32 ± 0.16	0.24 ± 0.14	0.67 ± 0.29
heavy	1.56 ± 0.28	1.39 ± 0.37	2.08 ± 0.55	1.32 ± 0.25	1.96 ± 0.49	1.82 ± 0.47	1.40 ± 0.25	1.31 ± 0.34	1.23 ± 0.25	1.64 ± 0.32
^a TALOS detects dynamics in the terminal residues										
^b Pairwise rms deviation was calculated among 20 structures of the peptide considering residues 2-9										

Table S3. Random coil chemical shifts of norleucine in the reference peptide *Ac-GGXGG-NH₂* measured in 7 M urea in D₂O at pH 2.3 or 7.4 (the peptide was synthesized by using the protocol reported above for the linear precursors of the lactam-bridged peptides **1Y**, **2-10**. Purity based on analytical HPLC: 95%. MS_{theor.}: 400.44, MS_{found} for M+Na⁺: 423.602 Da).

Resonance	δ (ppm)	
	pH 2.3	pH 7.4
C	177.8	177.7
C α	57.0	57.0
C β	33.3	33.4
C γ	30.1	30.1
C δ	24.4	24.5
C ϵ	15.9	15.9
H	8.24	8.25
H α	4.30	4.30
H β 2	1.82	1.82
H β 3	1.72	1.72
H γ	1.31	1.31
H δ	1.31	1.31
H ϵ	0.88	0.88

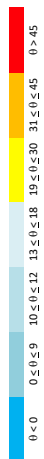
Table S4. Chemical shifts of the backbone amide protons (H^N) and $^3J_{HN\alpha}$ coupling constants of the lactam-bridged peptides in water (pH range 3-4). Values extrapolated from partially overlapped signals are in brackets (n.e.: not extractable. X = norleucine).

1Y		2		3		4					
δH^N (ppm)	$^3J_{HN\alpha}$ (Hz)	δH^N (ppm)	$^3J_{HN\alpha}$ (Hz)	δH^N (ppm)	$^3J_{HN\alpha}$ (Hz)	δH^N (ppm)	$^3J_{HN\alpha}$ (Hz)				
V	8.15	6.4	V	8.14	6.3	V	8.15	6.7	V	8.135	(6.4)
K	8.35	3.8	K	8.33	(4.8)	K	8.33	(4.4)	K	8.35	4.1
R	8.20	n.e.	R	8.25	3.8	R	8.26	4.5	R	8.24	4.2
L	7.39	n.e.	X	7.46	5.8	Y	7.47	7.4	L	7.44	n.e.
Q	8.20	n.e.	Q	8.22	5.1	Q	8.39	5.3	Q	8.14	(6.0)
D	8.27	6.5	D	8.33	(4.8)	D	8.33	(6.7)	D	8.15	(6.2)
L	7.67	6.0	L	7.78	5.6	L	7.86	6.4	I	7.68	6.6
Q	7.99	6.5	Q	8.03	(6.5)	Q	8.09	6.6	Q	8.15	(6.8)
Y	7.92	7.8	Y	7.95	7.8	Y	7.96	7.7	Y	8.09	7.9

5		6		7		8					
$\delta \alpha NH$ (ppm)	$^3J_{HN\alpha}$ (Hz)	$\delta \alpha NH$ (ppm)	$^3J_{HN\alpha}$ (Hz)	$\delta \alpha NH$ (ppm)	$^3J_{HN\alpha}$ (Hz)	$\delta \alpha NH$ (ppm)	$^3J_{HN\alpha}$ (Hz)				
Y	8.15	5.9	X	8.17	(5.7)	X	8.21	(5.6)	X	8.21	5.6
K	8.19	4.9	K	8.33	4.7	K	8.30	(3.6)	K	8.30	(4.8)
R	8.09	(4.5)	R	8.32	4.6	R	8.17	3.8	R	8.22	4.5
L	7.49	7.0	I	7.29	8.0	X	7.42	6.6	Y	7.45	7.5
Q	8.06	5.7	Q	8.18	(5.5)	Q	8.20	(5.6)	Q	8.36	5.3
D	8.14	7.3	D	8.26	6.9	D	8.30	(6.7)	D	8.30	(6.4)
V	7.75	6.7	V	7.82	6.8	X	7.68	5.8	L	7.84	6.2
Q	8.21	7.00	Q	8.22	6.9	Q	7.98	6.6	Q	8.16	6.8
Y	8.10	(7.7)	Y	8.11	8.0	Y	7.94	7.7	V	8.00	(8.0)

9		10			
$\delta \alpha NH$ (ppm)	$^3J_{HN\alpha}$ (Hz)	$\delta \alpha NH$ (ppm)	$^3J_{HN\alpha}$ (Hz)		
L	8.21	(5.5)	I	8.13	6.7
K	8.27	4.3	K	8.38	4.8
R	8.18	(4.4)	R	8.42	4.5
X	7.48	6.4	V	7.26	7.7
Q	8.20	(5.8)	Q	8.24	5.1
D	8.31	6.9	D	8.33	7.2
Y	7.87	6.2	Y	7.93	6.5
Q	8.12	7.0	Q	8.21	7.1
L	7.97	7.1	L	8.04	6.8

Table S5. Tilt angles θ and residues per turn calculated for residues 1-6 in all 20 low-energy structures of the lactam-bridged peptides **1Y**, **2-7**, **9** and **10**



0 < 0 0 ≤ 0 ≤ 9 10 ≤ 0 ≤ 12 13 ≤ 0 ≤ 18 19 ≤ 0 ≤ 30 31 ≤ 0 ≤ 45 0 > 45

33*: average of structures no. 1,2,7,8,17,18; 78*: average of structures no. 3,6,9,16,19,20

29*: average of structures no. 2,3,7,10,13,15,17,19; 72*: average of structures no. 1,4,6,11,12,14,18,10

24*: average of structures no. 2,6,8,9,11-14,16-18,23; 71*: average of structures no. 1,7,10,15

low-energy structure no.	1	2	3	4	5	6	7	8	9	10	11	12	13	14	15	16	17	18	19	20	Ave	Stdev	Ave	Stdev
1Y low-energy structure no.	4.2	4.2	4.2	4.1	4.1	4.2	4.2	4.1	4.2	4.2	4.2	4.2	4.2	4.2	4.2	4.2	4.2	4.2	4.2	4.2	4.2	4.2	4.2	0.0
Rho (residues/turn):	-14	-15	-17	-14	-14	-14	-17	-17	-13	-14	-13	-13	-13	-13	-14	-13	-12	-17	-14	-16	-14	2	2	
Theta(VAl2@CO):	20	21	19	18	17	17	18	21	15	14	14	14	13	13	14	15	12	14	15	12	14	16	3	
Theta(LV13@CO):	-1	-1	4	1	1	1	5	2	2	3	2	2	3	3	5	5	0	8	5	8	3	3	3	
Theta(AR6@CO):	17	15	20	18	21	20	14	23	22	23	22	22	23	23	24	23	16	9	24	24	20	4		
Theta(LV6@CO):	32	32	29	28	28	27	34	39	27	28	28	28	27	28	26	26	32	31	27	26	33	3	78	1
Theta(AS17@CO):	1	2	3	4	5	6	7	8	9	10	11	12	13	14	15	16	17	18	19	20	Ave <td>Stdev<td>Ave<td>Stdev</td> </td></td>	Stdev <td>Ave<td>Stdev</td> </td>	Ave <td>Stdev</td>	Stdev
2 low-energy structure no.	4.2	4.2	4.2	4.2	4.2	4.2	4.2	4.2	4.2	4.2	4.2	4.2	4.2	4.2	4.2	4.2	4.2	4.2	4.2	4.2	4.2	4.2	4.2	0.0
Rho (residues/turn):	-10	-10	-10	-9	-9	-9	-9	-9	-9	-9	-9	-9	-9	-9	-9	-9	-8	-8	-8	-8	-9	-9	1	
Theta(VAl2@CO):	10	10	10	10	10	10	10	7	8	8	7	8	8	7	7	6	10	7	6	10	7	10	8	1
Theta(LV13@CO):	-4	-4	-4	-4	-4	-4	-4	0	0	0	0	0	0	0	0	0	0	0	0	0	0	0	0	1
Theta(AR6@CO):	16	16	18	18	18	16	16	21	21	20	20	20	21	20	21	21	23	19	27	19	20	2		
Theta(LV6@CO):	32	32	31	31	32	32	26	27	26	26	26	26	27	27	27	27	26	28	28	22	28	2	3	
Theta(GLN6@CO):	67	67	67	67	68	68	66	66	65	65	65	65	65	65	66	66	68	68	69	68	66	65	65	1
Theta(AS17@CO):	1	2	3	4	5	6	7	8	9	10	11	12	13	14	15	16	17	18	19	20	Ave <td>Stdev<td>Ave<td>Stdev</td> </td></td>	Stdev <td>Ave<td>Stdev</td> </td>	Ave <td>Stdev</td>	Stdev
3 low-energy structure no.	4.2	4.2	4.2	4.2	4.2	4.2	4.2	4.2	4.2	4.2	4.2	4.2	4.2	4.2	4.2	4.2	4.2	4.2	4.2	4.2	4.2	4.2	4.2	0.0
Rho (residues/turn):	-10	-12	-11	-12	-12	-12	-12	-12	-12	-12	-12	-12	-12	-13	-12	-12	-12	-12	-12	-12	-12	-12	1	
Theta(VAl2@CO):	11	12	12	14	14	12	12	12	13	14	14	14	13	14	12	13	13	14	13	13	13	13	1	
Theta(LV13@CO):	16	17	19	19	19	19	21	21	21	21	21	21	21	20	20	22	21	21	21	19	20	2		
Theta(AR6@CO):	8	0	5	-1	-1	3	1	1	0	-1	0	-1	0	-1	5	0	0	-1	1	1	1	2		
Theta(LV6@CO):	26	24	26	26	26	26	27	27	27	26	29	29	27	27	27	28	27	30	26	27	27	1		
Theta(GLN6@CO):	71	31	26	73	73	73	29	27	30	30	71	71	27	73	26	31	70	71	30	72	29	2	72	1
Theta(AS17@CO):	1	2	3	4	5	6	7	8	9	10	11	12	13	14	15	16	17	18	19	20	Ave <td>Stdev<td>Ave<td>Stdev</td> </td></td>	Stdev <td>Ave<td>Stdev</td> </td>	Ave <td>Stdev</td>	Stdev
4 low-energy structure no.	4.2	4.2	4.2	4.2	4.2	4.2	4.2	4.2	4.2	4.2	4.2	4.2	4.2	4.2	4.2	4.2	4.2	4.2	4.2	4.2	4.2	4.2	4.2	0.0
Rho (residues/turn):	-11	-10	-9	-11	-9	-13	-9	-10	-11	-10	-10	-10	-10	-10	-10	-10	-11	-10	-11	-10	-11	-11	1	
Theta(VAl2@CO):	13	12	12	13	12	15	12	12	13	13	12	15	13	13	15	12	14	12	13	13	13	1		
Theta(LV13@CO):	0	0	0	1	3	0	0	0	0	0	0	3	2	2	3	0	5	0	5	6	1	2		
Theta(AR6@CO):	9	10	10	9	6	-3	10	9	10	9	10	-2	0	5	-4	9	6	9	6	9	6	6	5	
Theta(LV6@CO):	26	24	27	27	26	28	26	27	22	25	20	16	26	12	26	19	31	25	31	28	25	5		
Theta(GLN6@CO):	29	29	29	30	31	35	28	28	23	25	20	19	35	17	21	23	28	16	30	27	26	5		
Theta(AS17@CO):	1	2	3	4	5	6	7	8	9	10	11	12	13	14	15	16	17	18	19	20	Ave <td>Stdev<td>Ave<td>Stdev</td> </td></td>	Stdev <td>Ave<td>Stdev</td> </td>	Ave <td>Stdev</td>	Stdev
5 low-energy structure no.	4.3	4.3	4.3	4.4	4.3	4.3	4.3	4.3	4.3	4.4	4.3	4.3	4.3	4.3	4.3	4.3	4.3	4.3	4.3	4.3	4.3	4.3	4.3	0.0
Rho (residues/turn):	-16	-17	-17	-19	-14	-16	-18	-19	-17	-18	-18	-17	-18	-17	-18	-17	-17	-20	-16	-16	-17	2		
Theta(VR7@CO):	11	11	16	14	11	12	7	9	16	13	15	16	14	9	12	11	13	16	12	14	12	2		
Theta(LV13@CO):	31	31	19	34	31	30	28	27	19	32	18	19	38	34	35	29	30	19	31	20	28	6		
Theta(AR6@CO):	-1	-2	34	-6	1	-3	-1	-2	34	-3	34	33	-5	-3	-1	-2	-9	35	-2	33	-3	34	1	
Theta(LV6@CO):	54	25	32	30	33	35	34	38	37	32	31	31	35	34	37	37	38	37	30	34	3	3		
Theta(GLN6@CO):	76	27	22	28	24	24	74	24	17	71	20	23	28	26	64	22	29	17	35	23	24	4	71	5
Theta(AS17@CO):	1	2	3	4	5	6	7	8	9	10	11	12	13	14	15	16	17	18	19	20	Ave <td>Stdev<td>Ave<td>Stdev</td> </td></td>	Stdev <td>Ave<td>Stdev</td> </td>	Ave <td>Stdev</td>	Stdev

Table S5. Continued.

low-energy structure no.	1	2	3	4	5	6	7	8	9	10	11	12	13	14	15	16	17	18	19	20	Ave	Stdev	Ave	Stdev
Rhe (residues/turn):	4.2	4.2	4.2	4.2	4.2	4.2	4.2	4.2	4.2	4.2	4.2	4.2	4.2	4.2	4.2	4.2	4.2	4.2	4.2	4.2	4.2	4.2	4.2	4.2
Theat1L1Z@C(O):	13	5	4	39	3	49	3	27	24	55	15	38	49	23	41	4	11	40	4	27	8	5	37	11
Theat1LY3@C(O):	14	11	16	13	18	4	15	11	7	4	15	9	11	4	16	16	3	15	12	11	5			
Theat1ARGA@C(O):	26	29	20	26	46	20	30	19	28	13	25	22	23	24	20	27	30	22	33	20	25	4		
Theat1LE5@C(O):	8	10	6	7	3	23	5	8	5	23	6	14	12	9	24	-1	4	24	3	14	7	4	23	0
Theat1G1N6@C(O):	15	15	18	21	3	-4	7	6	-4	-4	16	11	11	14	-5	20	21	-9	23	12	14	6	-5	2
Theat1AS17@C(O):	43	50	41	41	35	44	46	43	37	44	44	43	47	44	44	37	54	42	38	54	44	5		
7 low-energy structure no.	1	2	3	4	5	6	7	8	9	10	11	12	13	14	15	16	17	18	19	20	Ave	Stdev	Ave	Stdev
Rhe (residues/turn):	4.2	4.2	4.2	4.2	4.2	4.2	4.2	4.2	4.2	4.2	4.2	4.2	4.2	4.2	4.2	4.2	4.2	4.2	4.1	4.2	4.2	4.2	4.2	4.2
Theat1NLEZ@C(O):	-14	-14	-14	-14	-14	-14	-12	-12	-12	-12	-12	-12	-12	-14	-9	-12	-9	-9	-3	-9	-11	3		
Theat1LY3@C(O):	24	24	24	23	24	23	14	14	14	14	15	15	20	21	15	24	23	7	7	10	13	3	23	1
Theat1ARGA@C(O):	6	6	6	6	7	7	10	10	10	9	9	9	12	8	11	5	5	4	4	11	8	3		
Theat1LE5@C(O):	6	5	6	5	5	5	4	4	4	4	4	4	4	4	4	3	2	2	2	2	1	22	1	
Theat1G1N6@C(O):	23	23	23	23	22	24	19	20	20	20	21	21	14	14	14	16	16	16	16	16	12	19	4	
Theat1AS17@C(O):	34	34	35	35	31	35	37	37	37	36	38	38	39	39	39	40	22	21	21	34	36	2		
9 low-energy structure no.	1	2	3	4	5	6	7	8	9	10	11	12	13	14	15	16	17	18	19	20	Ave	Stdev	Ave	Stdev
Rhe (residues/turn):	4.2	4.2	4.2	4.1	4.1	4.2	4.2	4.2	4.2	4.2	4.2	4.2	4.2	4.2	4.2	4.2	4.2	4.2	4.2	4.2	4.2	4.2	4.2	4.2
Theat1L1Z@C(O):	7	-10	-10	-7	-7	-9	-9	-9	-9	-9	-9	-9	-9	-9	-10	-10	-10	-10	-10	-10	-9	1		
Theat1LY3@C(O):	9	23	23	21	7	7	10	10	10	10	10	10	10	10	10	10	15	15	15	15	11	3	22	1
Theat1ARGA@C(O):	3	2	2	2	2	2	2	2	2	2	2	2	2	2	2	2	2	2	2	2	2	2	2	2
Theat1LE5@C(O):	23	19	19	19	19	19	18	18	18	18	18	18	18	18	18	18	16	16	16	16	18	1		
Theat1G1N6@C(O):	31	33	33	33	33	33	33	33	33	33	33	33	33	33	33	33	33	33	33	33	33	1	57	2
Theat1AS17@C(O):	39	42	42	42	36	37	35	35	35	35	35	35	35	35	35	36	36	36	36	34	36	37	3	
10 low-energy structure no.	1	2	3	4	5	6	7	8	9	10	11	12	13	14	15	16	17	18	19	20	Ave	Stdev	Ave	Stdev
Rhe (residues/turn):	4.4	4.2	4.2	4.4	4.2	4.2	4.6	4.4	4.4	4.2	4.2	4.2	4.2	4.2	4.2	4.2	4.2	4.2	4.2	4.1	4.2	4.3	4.1	4.2
Theat1LEZ@C(O):	38	42	3	40	56	55	39	41	41	59	40	47	48	42	40	-4	1	13	6	43	45	7		
Theat1LY3@C(O):	31	16	13	23	7	9	34	24	20	8	13	10	12	23	27	17	16	12	18	16	13	4	26	5
Theat1ARGA@C(O):	1	19	10	5	23	19	-7	5	5	23	9	20	10	6	-1	7	7	13	1	19	5	5	20	2
Theat1VAL5@C(O):	30	16	20	26	12	17	30	25	26	13	23	15	20	26	31	14	24	20	15	15	15	1	25	4
Theat1AS17@C(O):	34	42	34	35	46	39	33	35	35	45	33	48	32	33	34	33	34	33	34	33	34	37	6	

4*: average of all structures except no. 14,16,19. 22*: average of structures no. 14,16,19
 5*: average of all structures except no. 18,19
 6*: average of structures no. 1,3,5,7,11,16,17,19. 37*: average of structures no. 4,6,8,10,12,15,18,20
 7*: average of all structures except no. 6,10,15,18. 23*: average of structures no. 6,10,15,18
 8*: average of structures no. 1,3,5,7,11,16,17,19. 37*: average of structures no. 4,6,8,10,12,15,18,20
 9*: average of all structures except no. 5 and 10
 10*: average of all structures except no. 6,10,15,18. 23*: average of structures no. 6,10,15,18
 11*: average of all structures except no. 6,9,10,15,18. 5*: average of structures no. 6,9,10,15,18
 12*: average of all structures except no. 14,16,19
 13*: average of structures no. 7,12,15,18,20. 23*: average of structures no. 1,6,13,14,16,17
 14*: average of all structures except no. 14,16,19
 15*: average of structures no. 1,4,11. 57*: average of all structures except 1-4,11
 16*: average of structures no. 2,3,5,6,10,13,16,20. 26*: average of structures no. 1,4,7-9,14,15
 17*: average of structures no. 2,5,6,10,12,20. 33*: average of structures no. 1,3,4,7-9,11,13,19
 18*: average of all structures except 2,5,6,10,12,20. 20*: average of structures no. 2,5,6,10,12,20
 19*: average of structures no. 2,5,6,10,12,14,19,20. 25*: average of structures no. 1,3,4,7-9,11,13,15,17,18

Table S6. Tilt angles θ and residues per turn calculated for the lactam-bridged cyclized motifs from the crystal structures of Ac-(cyclo-2,6)-F(p-NO₂)KLLDF(p-NO₂)-NH₂ (CCDC deposition number 1941068⁶), Ac-(cyclo-6,10)-HKILHKLLQDS-NH₂ (PDB ID: 5WGD⁷), and Ac-(bicyclo-3,7+6,10)-HKS₅LHKS₅LQDS-NH₂ with S₅ = (S)-2-(4-pentenyl)Ala (PDB ID: 5WQG⁷).

Ac-(cyclo-2,6)-F(p-NO₂)KLLDF(p-NO₂)-NH₂ (CCDC deposition number 1941068⁶)

Rho (residues/turn):	4.2
Theta(PPN2@C,O):	7
Theta(LYS3@C,O): ^a	21
Theta(LEU4@C,O):	20
Theta(LEU5@C,O):	6
Theta(LEU6@C,O):	20
Theta(ASP7@C,O): ^a	29

^a lactam bridge

Ac-(cyclo-6,10)-HKILHKLLQDS-NH₂ (PDB ID: 5WGD⁷)

Chain	F	E
Rho (residues/turn):	4.0	4.0
Theta(ILE3@C,O):	14	11
Theta(LEU4@C,O):	10	22
Theta(HIS5@C,O):	5	15
Theta(LYS6@C,O): ^a	12	-6
Theta(LEU7@C,O):	26	38
Theta(LEU8@C,O):	15	
Theta(GLN9@C,O):	11	
Theta(ASP10@C,O): ^a	48	

^a lactam bridge

Ac-(bicyclo-3,7+6,10)-HKS₅LHKS₅LQDS-NH₂ with S₅ = (S)-2-(4-pentenyl)Ala (PDB ID: 5WQG⁷)

Chain	E	F
Rho (residues/turn):	4.0	3.9
Theta(LYS3@C,O):	23	24
Theta(MK84@C,O): ^a	5	21
Theta(LEU5@C,O):	4	10
Theta(HIS6@C,O):	25	18
Theta(LYS7@C,O): ^b	1	14
Theta(MK88@C,O): ^a	24	33
Theta(LEU9@C,O):	26	20
Theta(GLN10@C,O):	16	26
Theta(ASP11@C,O): ^b	42	-1
Theta(SER12@C,O):	58	

^a hydrocarbon bridge. ^b lactam bridge

References

1. Wishart, D. S., Bigam, C. G., Holm, A., Hodges, R. S., and Sykes, B. D. ^1H , ^{13}C and ^{15}N random coil NMR chemical shifts of the common amino acids. I. Investigations of nearest-neighbor effects. *J Biomol NMR*. 1995;5(1):67-81. <https://www.ncbi.nlm.nih.gov/pubmed/7881273>
2. Neukirchen, S., Krieger, V., Roschger, C., Schubert, M., Elsasser, B., and Cabrele, C. Impact of the amino acid sequence on the conformation of side chain lactam-bridged octapeptides. *J Pept Sci*. 2017;23(7-8):587-596. <https://onlinelibrary.wiley.com/doi/10.1002/psc.2997>
3. Roschger, C., Neukirchen, S., Elsasser, B., Schubert, M., Maeding, N., Verwanger, T., Krammer, B., and Cabrele, C. Targeting of a helix-loop-helix transcriptional regulator by a short helical peptide. *ChemMedChem*. 2017;12(18):1497-1503. <https://chemistry-europe.onlinelibrary.wiley.com/doi/10.1002/cmdc.201700305>
4. Roschger, C., Verwanger, T., Krammer, B., and Cabrele, C. Reduction of cancer cell viability by synergistic combination of photodynamic treatment with the inhibition of the Id protein family. *J Photochem Photobiol B*. 2018;178:521-529. <https://www.sciencedirect.com/science/article/pii/S1011134417312277?via%3Dihub>
5. Gautier, R., Douguet, D., Antony, B., and Drin, G. HELIQUEST: a web server to screen sequences with specific alpha-helical properties. *Bioinformatics*. 2008;24(18):2101-2102. <https://www.ncbi.nlm.nih.gov/pubmed/18662927>
6. Hoang, H. N., Wu, C., Hill, T. A., Dantas de Araujo, A., Bernhardt, P. V., Liu, L., and Fairlie, D. P. A novel long-range n to pi* interaction secures the smallest known alpha-Helix in water. *Angew Chem Int Ed*. 2019;58(52):18873-18877. <https://onlinelibrary.wiley.com/doi/10.1002/anie.201911277>
7. Speltz, T. E., Mayne, C. G., Fanning, S. W., Siddiqui, Z., Tajkhorshid, E., Greene, G. L., and Moore, T. W. A "cross-stitched" peptide with improved helicity and proteolytic stability. *Org Biomol Chem*. 2018;16(20):3702-3706. <https://doi.org/10.1039/C8OB00790J>